Generation of acoustic helical wavefronts using metasurfaces

Hussein Esfahlani[1,2], Herve Lissek[1], and Juan R. Mosig[2]

[1]Ecole Polytechnique Fédérale de Lausanne, Laboratoire de Traitement des Signaux LTS2, Lausanne, Switzerland.
[2]Ecole Polytechnique Fédérale de Lausanne, Laboratoire d'Electromagnétisme et d'Antennes LEMA, Lausanne, Switzerland.

October 8, 2016

Supplementary Notes

S-parameter retrieval

In the following, we will consider two cylindrical waveguides separated by a device under test (DUT) of thickness s, the scattering parameters of which will be assessed. A loudspeaker is used to generate sound in the first (incident) waveguide, the second waveguide being closed with an anechoic termination, and four microphones are placed at locations x_i at both sides of the interface to measure the sound pressures $P_i = P(x_i)$, as shown in Fig. (1). Mathematically, the pressures P_i are defined by:

$$P_1 = (ae^{-jkx_1} + be^{jkx_1})e^{j\omega t} \tag{1a}$$

$$P_2 = (ae^{-jkx_2} + be^{jkx_2})e^{j\omega t} \tag{1b}$$

$$P_3 = (ce^{-jkx_3} + de^{jkx_3})e^{j\omega t} \tag{1c}$$

$$P_4 = (ce^{-jkx_4} + de^{jkx_4})e^{j\omega t} \tag{1d}$$

where, k represents the wave number in the ambient fluid and an $e^{+j\omega t}$ sign convention has been adopted. The four complex pressures, P_1 to P_4, represent the superposition of two plane waves, travelling in opposite directions, as depicted in Fig. (1). The four wave amplitude coefficients (a, b, c, d) can be derived from Eq. (1a-1d) as functions of the four pressures :

$$a = \frac{j(P_1 e^{jkx_2} - P_2 e^{jkx_1})}{2sink(x_1 - x_2)} \tag{2a}$$

$$b = \frac{j(P_2 e^{-jkx_1} - P_1 e^{-jkx_2})}{2sink(x_1 - x_2)} \tag{2b}$$

$$c = \frac{j(P_3 e^{jkx_4} - P_4 e^{jkx_3})}{2sink(x_3 - x_4)} \tag{2c}$$

$$d = \frac{j(P_4 e^{-jkx_3} - P_3 e^{-jkx_4})}{2sink(x_3 - x_4)}. \tag{2d}$$

Let us look at the DUT as a 2-port, with "inward" sound pressures represented by ae^{-jkx} in the incident medium and de^{+jkx} in the transmission medium, and "outward" sound pressure represented by be^{jkx} and ce^{-jkx}. Then, the reflected waves amplitudes (b, c) can be related to the incident wave amplitudes (a, d) by the scattering matrix [S]. For the measurement setup described in Fig. (1), the corresponding matrix equations is:

$$\begin{pmatrix} b \\ ce^{-jks} \end{pmatrix}_{Refflected} = \begin{pmatrix} S_{11} & S_{12} \\ S_{21} & S_{22} \end{pmatrix} \begin{pmatrix} a \\ de^{jks} \end{pmatrix}_{Incident} \tag{3}$$

where s is the thickness of the sample.

To compute the four scattering parameters S_{ij}, two measurement configura-

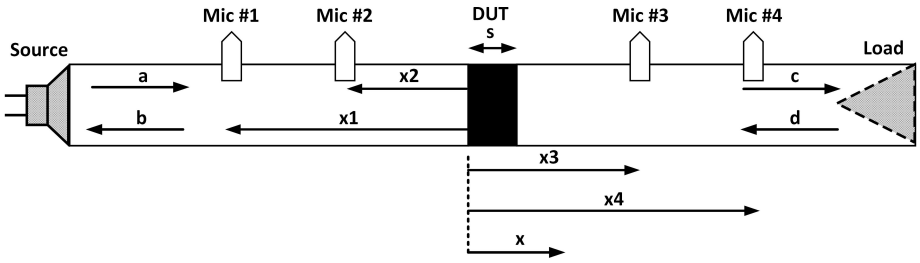

Figure 1: Schematic representation of four microphone measurement setup.

tions must be considered, corresponding to two different load conditions at the left and right termination of the waveguides, yielding two different sets of amplitudes (a_1, b_1, c_1, d_1) and (a_2, b_2, c_2, d_2). Then, the elements of the [S] matrix are given by:

$$S_{11} = \frac{b_1 d_2 e^{jks} - b_2 d_1 e^{jks}}{a_1 d_2 e^{jks} - a_2 d_1 e^{jks}} \tag{4a}$$

$$S_{12} = \frac{a_1 b_2 - a_2 b_1}{a_1 d_2 e^{jks} - a_2 d_1 e^{jks}} \tag{4b}$$

$$S_{21} = \frac{c_1 e^{-jks} d_2 e^{jks} - c_2 e^{-jks} d_1 e^{jks}}{a_1 d_2 e^{jks} - a_2 d_1 e^{jkl}} \tag{4c}$$

$$S_{22} = \frac{a_1 c_2 e^{-jks} - a_2 c_1 e^{-jks}}{a_1 d_2 e^{jks} - a_2 d_1 e^{jks}}. \tag{4d}$$

However, for symmetrical ($S_{11} = S_{22}$) and reciprocal ($S_{12} = S_{21}$) networks, the [S] matrix has only two different elements and a single measurement suffices. This is the case for proposed unit-cell where the [S] matrix is given by:

$$S_{11} = S_{22} = \frac{ab - cd}{a^2 - d^2 e^{2jks}} \tag{5a}$$

$$S_{12} = S_{21} = \frac{ace^{-jks} - bde^{jks}}{a^2 - d^2 e^{2jks}}. \tag{5b}$$

If an anechoic termination is used as a load, then $d = 0$ and the reflection and transmission coefficients R and T can be derived from equations 5a-5b:

$$R = S_{11} = S_{22} = \frac{b}{a} \tag{6}$$

$$T = S_{12} = S_{21} = \frac{c}{a} e^{-jks}. \tag{7}$$

Note that these coefficients are calculated whit respect to the two terminal planes of the sample $x = 0$ and $x = s$.

Figure. (2) shows a picture of the measurement setup used to retrieve the transmission coefficient of the helicoidal unit-cells.

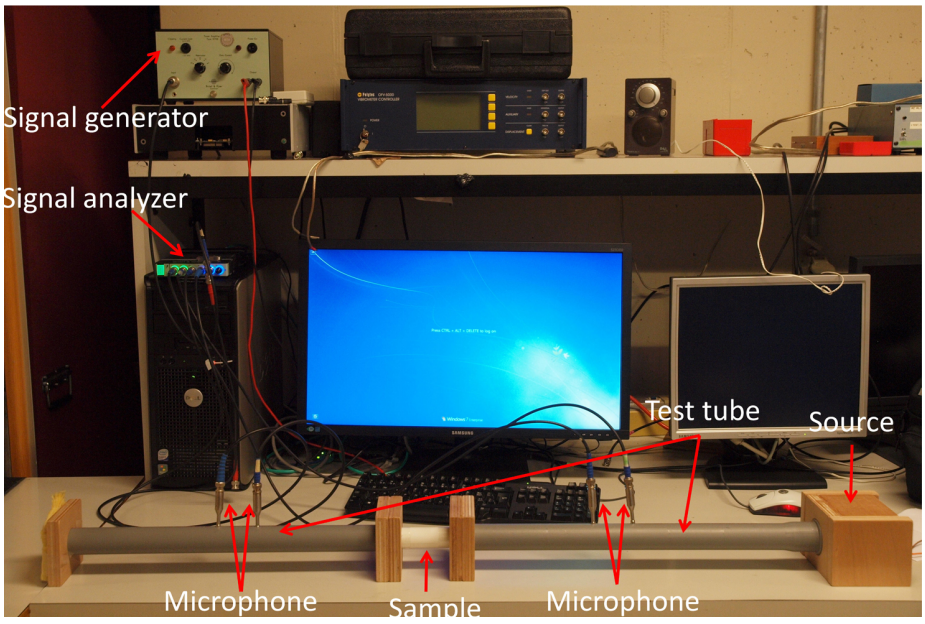

Figure 2: Four microphone measurement setup.

Transmitted, Reflected and Lost Power

Using the measurement procedure proposed in the preceding section, the reflection, transmission and lost power coefficients ($|R|^2$, $|T|^2$ and $\alpha = 1 - |R|^2 - |T|^2$) have been assessed on the 8 helicoidal unit-cells. As depicted in Fig. (3), the percentages of the reflected and lost power depend on the the number of helicoidal turns and increase as unit-cells density increases. While the designed unit-cells have been optimized for best impedance matching, the occurrence of unpredictable losses and reflections in the fabricated prototypes yields the observable discrepancies between the measurements and simulations of sound power transmission coefficient amplitudes (See Fig. 1 in the main manuscript). These discrepancies are relatively small for coarse unit-cells with few number of turns, for which the values of sound power reflection coefficients and losses are much lower than the transmitted one, and increase for denser unit-cells as highlighted by the higher values of reflections and losses. The effect of sound power reflections and losses can be linked to the following physical origins:

- Actual vs. simulated helicoid wall thickness:
  In the numerical simulation, the helicoidal and cylindrical walls are assumed to present a smooth and rigid surfaces and zero thicknesses. Therefore, the only Acoustic pressure field has been accounted for in the COMSOL simulations, where the internal walls of the structure are set to hard boundary conditions, yielding the wall vibration, and the thermoviscous losses have been intentionally discarded. This simplifications are justified by the difficulty to render the actual wall thickness in the geometrical rendering of COMSOL without paying the price of prohibitive computational costs, relative to meshing and numerical processing [1]. However, due to the 3D-printing technology employed for building the prototypes, the actually fabricated helicoidal and cylindrical walls present unpredictable porosity and are not smooth, with random surface states varying around average thickness of $0.5mm$ and $1mm$ respectively (considering the fabrication precision, each prototype present varying thicknesses around the average). Such construction tolerances result in increasing the frictions within channels, and also in making the walls vibrate under the incident sound field, thus transferring part of the incident acoustic energy into mechanical energy.
- Thermoacoustic losses not accounted for in the simulations:
  The thickness of the helicoidal walls are of the same order of magnitude as the width of the narrow acoustic paths, especially for the denser unit-cells, and it affects the transmission characteristics. Then, in addition to the disregarded porosity of the prototypes walls, the thermoviscous losses resulting from the ultra-thin labyrinthine pathways is the second dominating factor contributing to decreasing the transmission coefficient.
- Presence of residual powder in the prototypes:
  The SLS fabrication process results in leaving residual material powder

inside the channels of the labyrinthine paths . While almost all the residual powder can be blown away for coarse unit-cells using compressed air, it is difficult if not impossible for denser twisted shapes. Consequently the paths are not cleaned properly in denser unit-cells and the remaining powder can block the channels increasing sound power reflection and absorption.

The last identified sources of discrepancies are dominant for the denser unit-cells, and the whole mentioned problems are the consequences of the 3D printing technology.

The most straightforward way to minimize the influence of the aforementioned problems consists in increasing the global length of each unit-cell h while increasing the thickness, which results in reducing fabrication problems and errors due to the lower density of helicoidal turns, and consequently lower value of absorption and reflection. However, this solution presents the critical shortcoming of increasing the global thickness of the structure, which contradicts the metasurface denomination. Another option consists in choosing an alternative piecewise function $f(\tau)$ for the modulation of helicoid to decrease both the sound power reflection and lost power coefficients. This solution has not been investigated here however.

Instead, rather than focusing on achieving unitary sound power transmission coefficient on all unit-cells, which is finally not required to obtain a Bessel beam (doughnut shaped) with helical phase front, a uniform transmission coefficient among unit-cells can be targeted. This can be done by partially blocking the output of each unit-cell, to the price of a degradation of the overall transmission performance. Then, the proposed design still preserves the thickness criterion of acoustic metasurfaces, transforming an incident plane wave into a helicoidal wave, to the price of a relative deterioration of the efficiency in terms of power transmission.

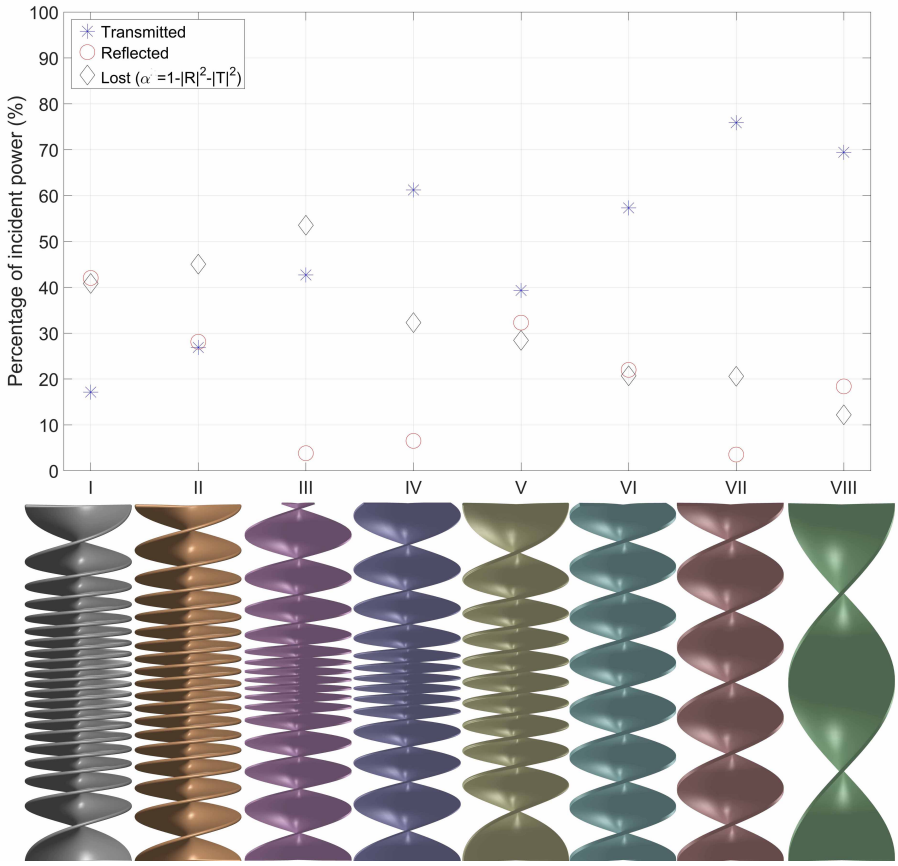

Figure 3: Measured transmitted, reflected and lost power in the helicoidal unit-cells.

Mathematical definitions of the proposed helicoidal unit-cells

The helicoid can be mathematically described as the following parametric equation:

$$\vec{r}(\rho, t) =< x, y, z >$$
$$=< \rho\, cos(2\pi \int_0^t f(\tau)d\tau),\ \rho\, sin(2\pi \int_0^t f(\tau)d\tau),\ b\, t >,$$

where ρ is the radius of helicoid, b is the constant rate of gradual displacement along z-axis, and for $b = 1$, t defines the height of the unit-cell. The spatial modulation function of the helicoid is $f(\tau) = f_c + f_\Delta x_m(t)$, where f_c is the average spatial frequency of twists, f_Δ is the deviation from f_c and $x_m(t)$ is a piecewise function allowing changing the spatial variations. Therefore, f_c controls the phase of the transmission coefficient, whereas f_Δ and x_m have an influence on the amplitude of the transmission coefficient, acting on the impedance matching. The mathematical definitions of the helicoidal unit-cells used for acoustic OAM have been summarized in Table. 1.

Table 1: Mathematical definitions of helcoidal Unit-cells.

Unit-cell	**d[mm]**	**h[mm]**	**N**	$\boldsymbol{f_c = \frac{N}{h}}$	$\boldsymbol{f_m = \frac{1}{h}}$	**k**	$\boldsymbol{f_\Delta = k(f_c - f_m)}$	$\boldsymbol{x_m(t)}$
I	30	100	10	0.1	0.01	0.9	0.081	$cos(2\pi f_m t)$
II	30	100	9	0.09	0.01	0.7	0.056	$cos(2\pi f_m t)$
III	30	100	7.8	0.078	0.01	1	0.068	$u(x) = \begin{cases} cos(2\pi\frac{2f_m}{3}t) & 0 < t < \frac{3h}{8} \\ cos(2\pi 2 f_m t + \pi) & \frac{3h}{8} < t < \frac{5h}{8} \\ cos(2\pi\frac{2f_m}{3}t + \frac{2\pi}{3}) & \frac{5h}{8} < t < h \end{cases}$
IV	30	100	6.6	0.066	0.01	1	0.056	$c(t)$
V	30	100	5	0.05	0.01	0.9	0.036	$cos(2\pi f_m t)$
VI	30	100	3.6	0.036	0.01	0.1	0.0026	$cos(2\pi f_m t)$
VII	30	100	2.5	0.025	0.01	0	0	$cos(2\pi f_m t)$
VIII	30	100	1	0.01	0.01	0	0	$cos(2\pi f_m t)$

$$\vec{r}(\rho,t) =< x, y, z >, \begin{cases} x = \rho cos(2\pi \int_0^t f(\tau)d\tau) = \rho cos(2\pi \int_0^t [f_c + f_\Delta x_m(t)]d\tau) = \rho cos(2\pi f_c t + 2\pi f_\Delta \int_0^t x_m(t)d\tau) & 0 < t < h \\ y = \rho sin(2\pi \int_0^t f(\tau)d\tau) = \rho sin(2\pi \int_0^t [f_c + f_\Delta x_m(t)]d\tau) = \rho sin(2\pi f_c t + 2\pi f_\Delta \int_0^t x_m(t)d\tau) & -\frac{d}{2} < \rho < \frac{d}{2} \\ z = bt & b = 1 \end{cases}$$

Measurement setup for the OAM Metasurface

The measurement setup for our proposed acoustic OAM is shown in Fig. 4 and the corresponding dimensions have been summarized in Table. 2.

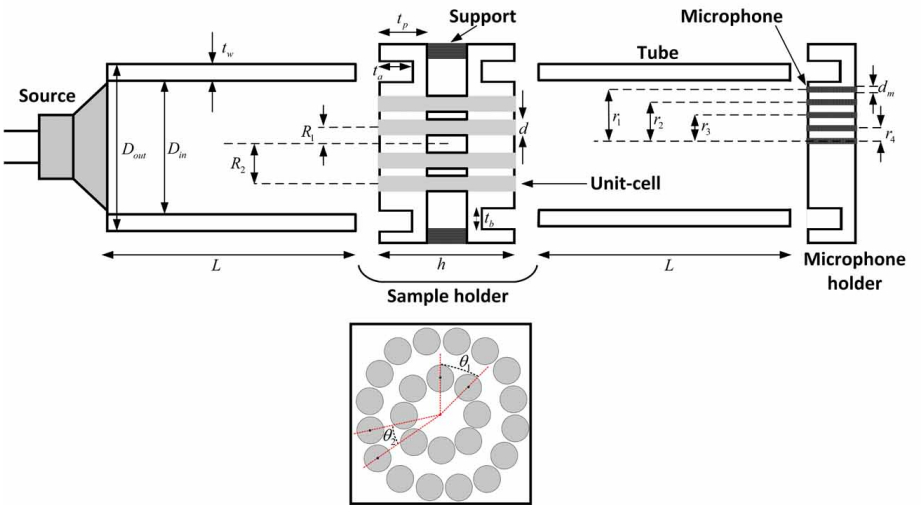

Figure 4: Schematic representation of the acoustic OAM measurement setup.

Table 2: OAM measurement setup dimensions.

Symbol	Value (mm)	Symbol	Value (mm)
D_{out}	200	h	100
D_{in}	194	θ_1	45^o
t_w	3	θ_2	22.5^o
t_b	3.5	R_1	45
t_a	4	R_2	81.50
t_p	8	r_1	88
d	30	r_2	66
d_m	7	r_3	44
L	800	r_4	22

The diameter of the holes holding the unit-cells is chosen to be $0.8mm$ bigger than $d = 30mm$ (unit-cell diameter) in order to fit the helicoidal unit-cells in the support holes.

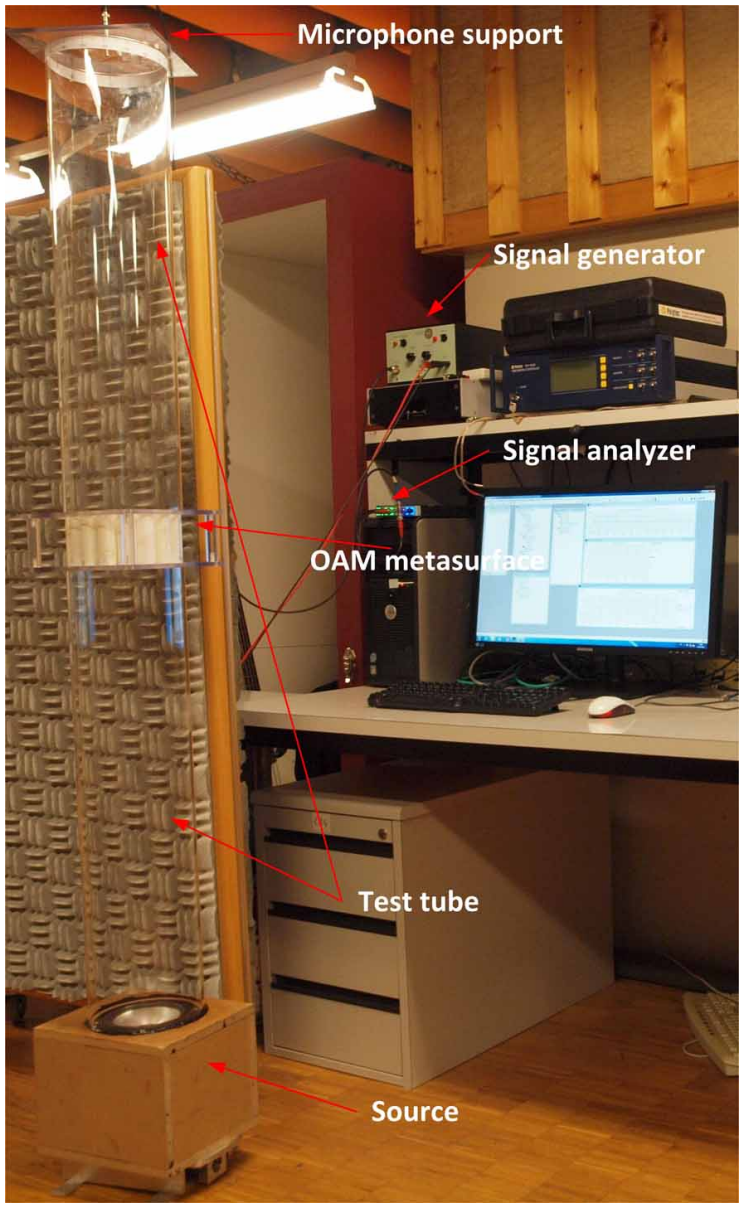

Figure 5: Acoustic OAM measurement setup.

References

[1] https://www.comsol.com/blogs/how-to-model-thermoviscous-acoustics-in-comsol-multiphysics/

[2] https://www.comsol.com/blogs/theory-of-thermoviscous-acoustics-thermal-and-viscous-losses/